Vol 17 No 7, July 2008
1674-1056/2008/17(07)/2639-07

Chinese Physics B

© 2008 Chin. Phys. Soc.
and IOP Publishing Ltd

Electronic structure and thermodynamic properties of LiBC under high pressure*

Ai Qiong(艾 琼)[a)b)], Fu Zhi-Jian(付志坚)[a)],
Cheng Yan(程 艳)[b)], and Chen Xiang-Rong(陈向荣)[a)b)c)†]

[a)] *Institute of Atomic and Molecular Physics, Sichuan University, Chengdu* 610065, *China*
[b)] *College of Physical Science and Technology, Sichuan University, Chengdu* 610064, *China*
[c)] *International Centre for Materials Physics, Chinese Academy of Sciences, Shenyang* 110016, *China*

(Received 30 September 2007; revised manuscript received 21 January 2008)

This paper investigates the electronic structure and thermodynamic properties of LiBC in the hexagonal structure by using the generalized gradient approximation (GGA) and local density approximation correction scheme in the frame of density functional theory. The geometric structure of LiBC under zero pressure, and the dependences of the normalized lattice parameters a/a_0 and c/c_0, the ratio c/a, the normalized primitive volume V/V_0 on pressure are given. The thermodynamic quantity (including the heat capacity C_V, Debye temperature $\Theta_{\rm D}$, thermal expansion α and Grüneisen parameter γ) dependences on temperature and pressure are obtained through the GGA method and the quasi-harmonic Debye model. The band structures and density of state of LiBC under different pressures have also been analysed.

Keywords: thermodynamic properties, electronic structure, density functional theory, LiBC
PACC: 6740K, 7120H, 7115M

1. Introduction

The compound LiBC was first synthesized in 1995 by Wörle *et al* [1] who provided the crystal structure and reported the conductivity of hole-doping of Li atoms. It crystallizes in the hexangular structure with space group P63/mmc. In 2001, the discovery of high critical temperature $T_{\rm c} \sim 40\,{\rm K}$ superconductivity in MgB_2[2] has inspired the extensive work on similar properties of LiBC and other closely related intermetallic compounds, which is structurally similar to MgB_2.

In 2002, the hole-doped Li_xBC has been predicted to achieve higher transition temperature of $T_{\rm c} \sim 100\,{\rm K}$ (x=0.5).[3] Since then, a few investigations on the properties of LiBC, including lattice dynamics,[4,5] electronic and optical properties,[6–8] vibrational properties,[9–11] elastic properties,[12] and high pressure properties,[13] have come to the fore theoretically and experimentally. Recently attentions are centralized on how to produce an insulator–metal transition and possible superconductivity, one way is by metal-doping,[14] and the other is applying pressure[15] which is not successful experimentally.

Hinks *et al* [16] proposed that the electron–phonon coupling plays an important role in the superconductivity of LiBC. Electron–phonon coupling parameter λ increases monotonically with decreasing x to a maximum value of 1.4 for x=0.125 and thus results in $T_{\rm c} \sim 65\,{\rm K}$.[5] The DC resistivity and AC dielectric measurements[6] showed a strong anisotropy of the electrical transport properties in LiBC. Hlinka *et al* found that the polarized Raman measurements on the as-grown LiBC crystal were incompatible with its assumed $D_{6\rm h}$ symmetry and the sample was sensitive to heating to temperature exceeding 400 K.[7] Infrared reflectivity and micro-Raman scattering spectra of LiBC confirmed the prediction of large Born effective charges on the nodes of B–C grapheme sheets.[8] The extreme thermal expansion anisotropy in LiBC was observed by the high-resolution x-ray powder diffraction.[9]

In this work, we only focus on the electronic structure and thermodynamic properties of LiBC under pressure. We perform the electronic structure calculations using the full potential linearized augmented plane waves (FP-LAPW) in the frame of density functional theory (DFT). The structural, thermodynamic

*Project supported by the National Natural Science Foundation of China (Grant Nos 10776022 and 10576020).
†Corresponding author. E-mail: xrchen@126.com

and electronic properties of LiBC obtained are in good agreement with the available experimental data and other theoretical results. In Section 2, we give a brief description of the theoretical computational method. The results of structural, thermodynamic and electronic properties are presented and analysed in Section 3. Conclusion is drawn in the last Section.

2. Computational method

2.1. Total energy electronic structure calculations

Our calculations are carried out by means of the FP-LAPW in the frame of DFT[17,18] implemented in WIEN2K package.[19] In this method, the space is divided into an interstitial region (IR) and non-overlapping Muffin-tin (MT) atomic spheres centred at the atomic sites. In the IR region, the basis set consists of plane waves. Inside the MT spheres, the basis set is described by radial solutions of the one particle Schrödinger equation (at fixed energy) and their energy derivatives multiplied by spherical harmonics. In structural calculations, we perform the volume optimization both within the generalized gradient approximation (GGA)[20] and the local density approximation (LDA).[21] In the structural calculations, $R_{\rm MT}$ are taken to be 2.18 a.u., 1.46 a.u. and 1.46 a.u. for Li, B and C, respectively.

Because of big volume change under high pressure, we change $R_{\rm MT}$ to 1.70 a.u., 1.14 a.u. and 1.14 a.u. for Li, B and C atoms, respectively, to get good results. We expand the basis function up to $R_{\rm MT}K_{\rm max}$=7.0, where $K_{\rm max}$ is the largest reciprocal vector used in the LAPW basis set. The Brillouin zone is sampled on an uniform mesh with 1600 irreducible k-points. The energy convergence criterion is set to 0.1 mRy.

2.2. Quasi-harmonic Debye model

The quasi-harmonic Debye model,[22] in which the phononic effect is considered, is applied to investigate the thermodynamic properties of LiBC. In the quasi-harmonic Debye model, the non-equilibrium Gibbs function $G^*(V;P,T)$ can be written in the form of

$$G^*(V;P,T) = E(V) + PV + A_{\rm Vib}(\Theta(V);T), \quad (1)$$

where $E(V)$ is the total energy per unit cell, PV corresponds to the constant hydrostatic pressure condition, $\Theta(V)$ is the Debye temperature, the vibrational Helmholtz free energy $A_{\rm Vib}$ can be written as[23,24]

$$A_{\rm Vib}(\Theta;T) = nkT\left[\frac{9}{8}\frac{\Theta}{T} + 3\ln(1-{\rm e}^{-\Theta/T}) - D(\Theta/T)\right], \quad (2)$$

where $D(\Theta/T)$ represents the Debye integral, n is the number of atoms per formula unit. For an isotropic solid, Θ is expressed by

$$\Theta = \frac{\hbar}{k}\left[6\pi^2 V^{1/2} n\right]^{1/3} f(\sigma)\sqrt{\frac{B_{\rm S}}{M}}, \quad (3)$$

where M is the molecular mass, n is the number of atoms per formula unit, $B_{\rm S}$ is the adiabatic bulk modulus, which is approximated by the static compressibility [25,26]

$$B_{\rm S} \cong B(V) = V\left\{\frac{{\rm d}^2 E(V)}{{\rm d}V^2}\right\}, \quad (4)$$

where $f(\sigma)$ is given by Refs.[27, 28], the Poisson ratio σ is taken as 0.3. For the LiBC, n=3, M=29.762 a.u., thus the non-equilibrium Gibbs function $G^*(V;P,T)$ as a function of $(V;P,T)$ can be minimized with respect to volume V

$$\left(\frac{\partial G^*(V;P,T)}{\partial V}\right)_{P,T} = 0. \quad (5)$$

By solving Eq.(5), one can get the thermal equation of state (EOS). The heat capacity C_V and the thermal expansion coefficient α are given by[28]

$$B_{\rm T}(P,T) = V\left(\frac{\partial^2 G^*(V;P,T)}{\partial V^2}\right)_{P,T}, \quad (6)$$

$$C_V = 3nk_{\rm B}\left[4D(\Theta/T) - \frac{3\Theta/T}{{\rm e}^{\Theta/T}-1}\right], \quad (7)$$

$$\alpha = \frac{\gamma C_V}{B_T V}, \quad (8)$$

where γ is the Grüneisen parameter, which is defined as

$$\gamma = -\frac{{\rm d}\ln\Theta(V)}{{\rm d}\ln V}. \quad (9)$$

Through the quasi-harmonic Debye model, one could obtain the thermodynamic quantities of LiBC under pressure. By this method, we have successfully investigated on some materials.[29−33]

3. Results and discussion

3.1. Geometric structure and equation of state

For the hexagonal structure LiBC, the initial structural model is built according to previous available lattice parameters a and c. The lithium atom is set at (0, 0, 0), the boron atom at (1/3, 2/3, 1/4), and the carbon atom at (1/3, 2/3, 3/4). In the equilibrium geometry calculations, we change lattice parameter a with constant c/a to perform volume optimization both in GGA and LDA methods, respectively. Relativistic effects are taken into account within the scalar-relativistic approximation. The obtained results are listed in Table 1, together with the available experimental data[1,5,16] and other theoretical results.[12,13] The equilibrium lattice parameters obtained are well consistent with experiments.[16] Obviously, GGA method gives better geometrical parameters than LDA method. It is well known that LDA method often overestimates the binding energy, and underestimates the bond length by 1%–2%, which results in the calculated equilibrium volume normally 3%–6% less than experiments, and GGA method usually overestimates the lattice constants and underestimates the bulk module.

Table 1. Calculated and experimental equilibrium structural parameters of LiBC at 0 GPa and 0 K.

	c /nm	a/nm	c/a	B_0/GPa	B_0'
GGA (Present)	0.7050	0.2750	2.560	175.58	3.79
LDA (Present)	0.6853	0.2720	2.520	197.09	3.55
GGA [12]	0.6993	0.2756	2.537	180.10	3.66
LDA [12]	0.6894	0.2735	2.521	155.30	2.92
Ref.[13]	0.6870	0.2730	2.520		
Exp.[1]	0.7058	0.2752	2.565		
Exp.[5]	0.7053	0.2749	2.566		
Exp.[16]	0.7050	0.2750	2.560		

By fitting the corresponding $E-V$ data to the spinodal EOS proposed by Baonza *et al* [34]

$$V = V_{\rm sp}\exp\left\{-\left[\frac{K^*}{1-\beta}\right](p-p_{\rm sp})^{1-\beta}\right\}, \qquad (10)$$

$$V_{\rm sp} = V_0\exp\left\{\frac{\beta}{(1-\beta)B_0'}\right\}, \qquad (11)$$

where $P_{\rm sp}$ and $V_{\rm sp}$ are the spinodal pressure and volume, respectively, $P_{\rm sp}$, K^*, and β are the fitting parameters (it is customary to use β=0.85), we obtain the isothermal bulk modulus B_0 and its pressure derivative B_0' of LiBC at P=0 and T=0, which are also listed in Table 1 together with other theoretical results.[12] It is found that by using LDA method the bulk modulus B_0 and its pressure derivative B_0' are about 27% and 21% larger than those obtained from the full-potential linearized muffin-tin orbital method respectively by Liu *et al*,[12] while using GGA method the bulk modulus B_0 is slightly lower and its pressure derivative B_0' is slightly larger than those by Liu *et al*.[12] In the following, we will only apply GGA method for our calculations.

The pressure dependence of the normalized lattice parameters a/a_0 and c/c_0, the axial ratio c/a, and the normalized volume V/V_0 of LiBC are illustrated in Fig.1, where a_0, c_0 and V_0 are the zero-pressure equilibrium lattice parameters and the primitive-cell volume respectively, P is the pressure in GPa. It is shown that the compression along the c-axis is considerably larger than that along the a-axis in the basal plane. As pressure increases from 0 to 550 GPa, the c/a ratio decreases by 34.89%. The interlayer linear compressibility, $\mathrm{d}(\ln c)/\mathrm{d}P$=0.00231 GPa^{-1} is about

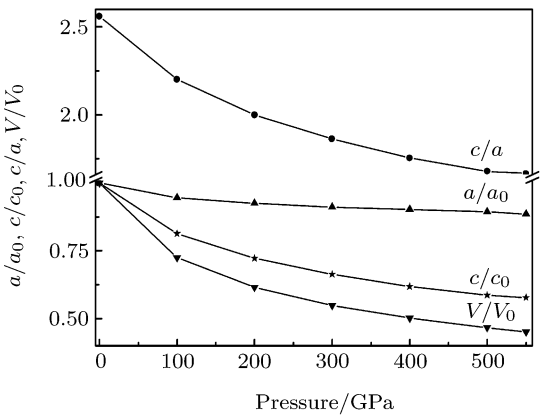


Fig.1. Ratios of a/a_0, c/c_0, c/a, and V/V_0 of LiBC versus pressure at 0 K.

3.467 times the basal plane value, $\mathrm{d}(\ln a)/\mathrm{d}P = 0.000666248\,\mathrm{GPa}^{-1}$. It means that the lattice constant c is more sensitive to pressure than the lattice constant a, this is consistent with the comparatively weaker Li–B bonds and Li–C bonds which determine the interlayer distance together.

3.2. Thermodynamic properties

The isothermal bulk modulus is defined by

$$B_T(P,T) = -V\left(\frac{\partial P}{\partial V}\right)_T. \tag{12}$$

From Eq.(12), we have B_0=179.93 GPa (T=0), this is well consistent with B_0=175.58 obtained by the spinodal EOS.[34] By fitting the $B-T$ data to a fourth-order polynomial, we have the following relation (P=0 GPa)

$$\begin{aligned} B_0 =& 179.93 - 0.00448T - 2.62857\times10^{-5}T^2 \\ &+ 1.59078\times10^{-8}T^3 - 3.89278\times10^{-12}T^4. \end{aligned} \tag{13}$$

Obviously, B_0 decreases as temperature T increases. When $T < 100$ K, B_0 decreases slowly; when $T >$100 K, B_0 decreases dramatically as T increases. The relationship between bulk modulus B and pressure P at different temperatures T=0, 600, 1800 K are shown in Fig.2. They are all nearly linear. The bulk modulus increases with pressure at a given temperature and decreases with temperature at a given pressure. All these results suggest that increasing pressure has exactly the opposite effect on the bulk modulus of materials as increasing temperature does. This result can be easily understood from the quasi-harmonic Debye model. The obtained $B-P$ curves show the weak temperature dependence for LiBC.

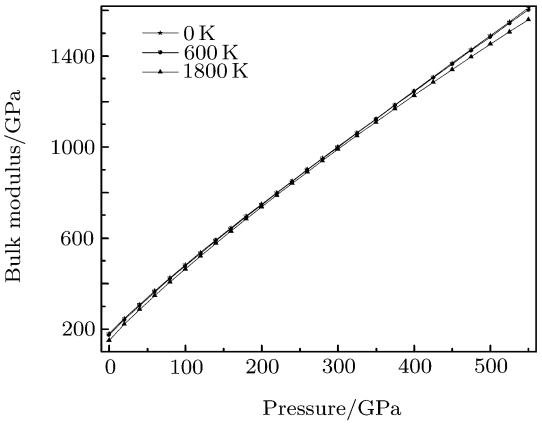


Fig.2. Bulk modulus of LiBC versus pressure at 0, 600, and 1800 K, respectively.

The obtained Debye temperatures at various temperatures (300, 800, 1300, 1500 and 1800 K) and pressures (0, 100, 200, 300, 400 and 500 GPa) are listed in Table 2. It is found that, when the temperature is constant, as pressure increases, the heat capacity C_V

Table 2. Some thermodynamic quantities of LiBC over a wide range of temperatures T and pressures P.

T/K		P/GPa					
		0	100	200	300	400	500
300	C_V	53.38102	35.59630	26.77860	21.35055	17.70467	15.08760
	Θ_D	808.92	1255.98	1527.58	1735.05	1904.69	2049.91
	α	1.74839682	0.44989883	0.23699352	0.14894857	0.10339455	0.07646437
	γ	1.624	1.232	1.141	1.074	1.021	0.977
800	C_V	71.27013	66.43091	62.83784	59.85366	57.30545	55.07495
	Θ_D	794.08	1250.45	1523.71	1732.08	1902.33	2047.87
	α	2.51453430	0.84640717	0.55921717	0.41925134	0.33557116	0.27958954
	γ	1.663	1.234	1.143	1.075	1.021	0.977
1300	C_V	73.51324	71.51570	69.96433	68.61686	67.41935	66.33007
	Θ_D	776.29	1243.56	1518.50	1727.78	1898.74	2045.23
	α	2.85350870	0.91861126	0.62623716	0.48275968	0.39604626	0.33728818
	γ	1.715	1.236	1.144	1.076	1.022	0.978
1500	C_V	73.85804	72.33206	71.14254	70.10202	69.17125	68.32022
	Θ_D	768.34	1240.71	1516.31	1725.94	1897.16	2043.76
	α	3.00113417	0.93213667	0.63822251	0.49404207	0.40680849	0.34767580
	γ	1.740	1.237	1.145	1.077	1.023	0.978
1800	C_V	74.17531	73.09470	72.25252	71.51091	70.84338	70.23027
	Θ_D	755.67	1236.37	1512.95	1723.14	1894.76	2041.53
	α	3.26131926	0.94652438	0.65040411	0.50529013	0.41740929	0.35784760
	γ	1.784	1.239	1.146	1.078	1.024	0.979

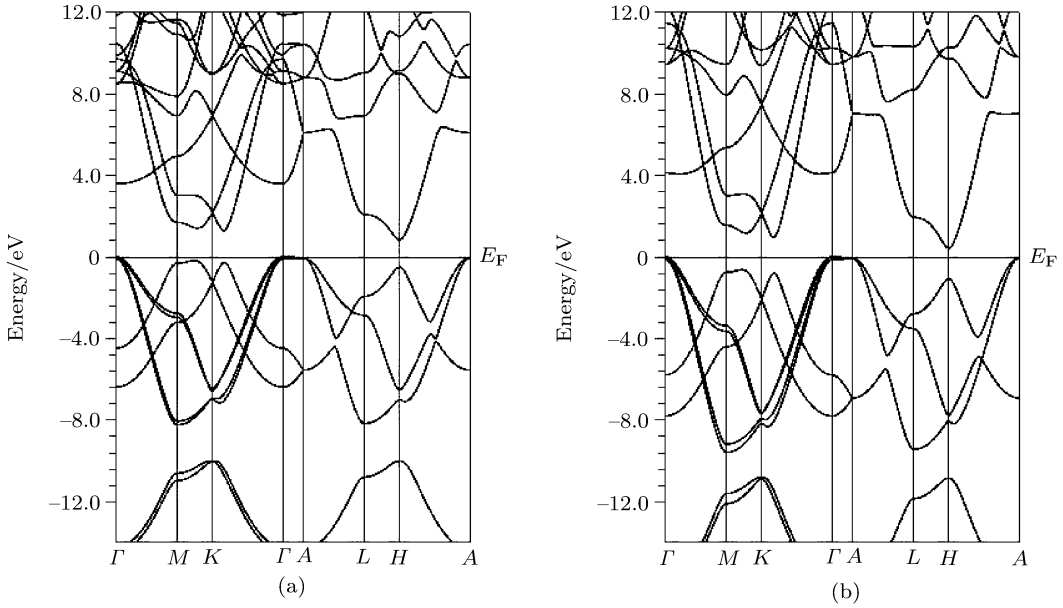
decreases, and the Debye temperature Θ_D increases. When the applied pressure increases from 0 to 500 GPa, the heat capacity C_V decreases by 71.74%, 22.72%, 12.49 %, 7.50 %, 5.32% at T = 300, 800, 1300, 1500 and 1800 K, respectively. When the applied temperature increases from 300 to 1800 K, the Debye temperature Θ_D decreases by 6.583%, 1.561%, 0.958%, 0.628%, 0.524% and 0.409% at 0, 100, 200, 300, 400 and 500 GPa, respectively. The heat capacity C_V in this work is 808.92J·mol^{-1}·K^{-1} at zero pressure and ambient temperature. We can find that C_V increases quickly at low temperature, and then becomes smoothly at high temperature, and is close to the Dulong–Petit limit C_V=9Nk_B, where N represents the Avogadro's constant.

Thermal expansion parameters are important for predicting thermodynamic properties. Thus in this work we also present the thermal expansion coefficient α of LiBC under various temperatures (300, 800, 1300, 1500 and 1800 K) and pressures (0, 100, 200, 300, 400 and 500 GPa). The thermal expansion coefficient of LiBC at a given temperature decreases swiftly with increasing pressure up to 100 GPa, then trends to a constant. Under a given pressure, α increases dramatically below 400 K and then gradually approaches to a linear increase at higher temperatures.

Another important thermodynamic quantity is the Grüneisen parameter γ, which can describe the vibration of volume by pressure changes. It has been widely used to characterize and extrapolate the thermodynamic properties of materials at high pressures and high temperatures. In Table 2, we present the Grüneisen parameter γ of LiBC under various pressures and temperatures. In the range of temperature from 0 K to 1800 K, the Grüneisen parameter γ shows the weak temperature dependence for LiBC.

3.3. Electronic structure properties

The band structure of LiBC at 0 K and 0 GPa (a/a_0=1) along high symmetry lines in the Brillouin zone is shown in Fig.3(a). The valence bands are separated from the conduction bands by a calculated gap of 0.856 eV, with the valence band maximum occurring at Γ, and the conduction band minimum occurring at H. At zero pressure, it bears many similarities to that of MgB_2. They both have nearly flat bands of $p\sigma$ character at the top of the valence bands between Γ and A as well as bonding and anti-bonding $p\sigma$ bands near the Fermi level (which cross it, to form Fermi surface "webbed tunnels" in the case of MgB_2) near the M and K regions.[15,35] For MgB_2, these two Fermi surface features are characterized by different superconducting energy gaps, making it a two-band superconductor with a transition temperature of 39 K.[36]



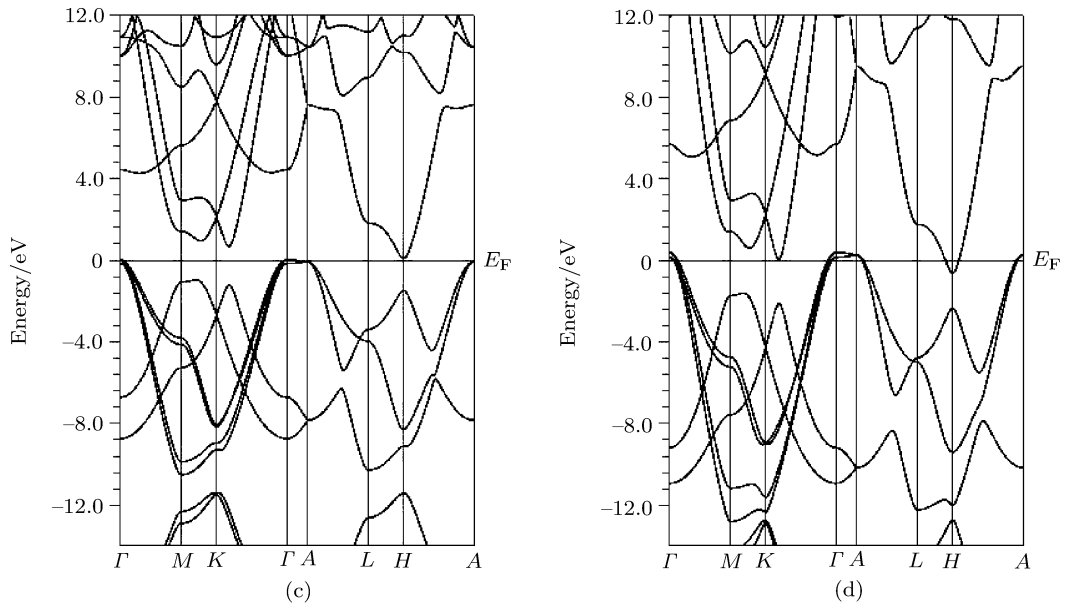


Fig.3. Band structures of LiBC at various pressures: (a) 0 GPa, (b) 60 GPa, (c) 120 GPa, and (d) 400 GPa.

LiBC is shown experimentally to remain stable crystal structure at ambient pressure up to at least 60 GPa.[15] As pressure increases from 0 to 60, 120 and 400 GPa , the corresponding c/a changes from 1 to 0.8, 0.7 and 0.5, and the calculated Fermi-levels are 0.45811, 0.64475, 0.76242 and 1.13386 (in Ry), respectively. The band structures show little difference below 60 GPa (corresponding to a/a_0=0.80). The occupied $p\sigma$ bands drop in energy with respect to the C π bands, losing their flatness between Γ and A, and dropping even further below the Fermi level. The unoccupied $p\pi$ bands drop in energy at L and H, while increase between Γ and M and between Γ and K, and finally overlap to become semimetallic at 120 GPa (corresponding to a/a_0=0.70). This is an indirect gap closure, and the direct gap near M and K becomes larger under pressure. After metallization, the density of states at the Fermi level increases rather rapidly, but none of these states come from the σ bands, which are of primary importance for superconductivity in the case of MgB_2. The examination of the electronic behaviour alone indicates that we are very unlikely to see that LiBC becomes superconducting under pressure experimentally. We list the band gap corresponding to band structure in Table 3. It is found that the indirect band gap becomes smaller with pressure, while the direct band gap becomes larger.

Table 3. Calculated band gap (in eV) of LiBC at various pressures P (GPa).

P/GPa	0	60	120	400
Direct (H)	1.352	1.501	1.579	1.740
Indirect (ΓH)	0.856	0.431	0.092	0

To further elucidate the nature of the electronic band structure, we have also calculated the total density of states (TDOS) of LiBC by using the modified tetrahedron method.[37] We should emphasize that

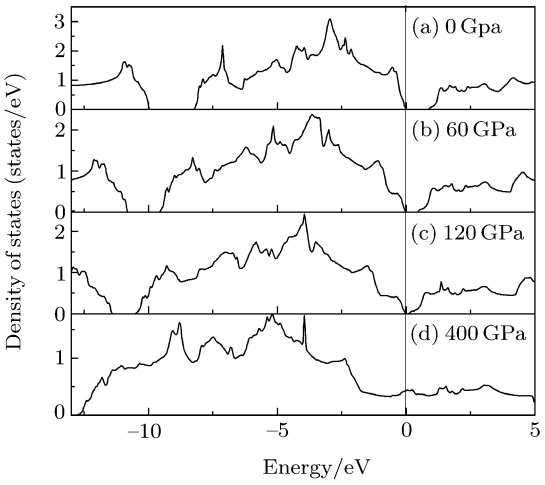


Fig.4. Density of states of LiBC at various pressures: (a) 0 GPa, (b) 60 GPa, (c) 120 GPa, and (d) 400 GPa.

there are three distinct structures in the density of states separated by gaps at 0 GPa. We give a compare of TDOS under different pressures in Fig.4. It is found that the gap near Fermi level narrows at 60 GPa, nearly disappears at 120 GPa and then links to a whole at 400 GPa. We can also find that the gap at valence bands becomes narrower and locomotes left with increasing pressure. These characters can easily be found from the electronic band structure.

4. Conclusion

We have determined the equilibrium structural parameters of LiBC under zero pressure and high pressure both in the GGA and LDA. The calculated lattice constants agree well with other theoretical results and the available experimental data. The obtained dependences of the normalized lattice parameters a/a_0 and c/c_0, ratio c/a, normalized primitive volume V/V_0 on pressure show that the lattice constant c is more sensitive to pressure than the lattice constant a, this is consistent with the comparatively weaker Li–B bonds and Li–C bonds which determine the interlayer distance together. The bulk modulus B, variation of heat capacity $C_{\rm V}$, Debye temperature $\Theta_{\rm D}$ and thermal expansion α under high temperature and high pressure are also discussed. At last, we have examined and analysed the band structure and the density of state for LiBC under pressure.

References

[1] Wörle M, Nesper R, Mair G, Schwarz M and von Schnering H G 1995 *Z. Anorg. Allg. Chem.* **621** 1153

[2] Nagamatsu J, Nakagawa N, Muranaka T, Zenitani Y and Akimutsu J 2001 *Nature* **410** 63

[3] Rosner H, Kitaigorodsky A and Pickett W E 2002 *Phys. Rev. Lett.* **88** 127001

[4] Renker B, Schober H, Adelmann P, Schweiss P, Bohnen K P and Heid R 2004 *Phys. Rev.* B **69** 52506

[5] Dewhurst J K, Sharma S, Ambrosch-Draxl C and Johansson B 2003 *Phys. Rev.* B **68** 20504(R)

[6] Pronin A V, Pucher K, Lunkenheimer P, Krimmel A and Loidl A 2003 *Phys. Rev.* B **67** 132502

[7] Hlinka J, Gregora I, Pokorný J, Pronin A V and Loidl A 2003 *Phys. Rev.* B **67** 020504

[8] Hlinka J, elezný V Ž, Gregora I, Pokorný J, Fogg A M, Claridge J B, Darling G R and Rosseinsky M J 2003 *Phys. Rev.* B **68** 220510(R)

[9] Fogg A M, Chalker P R, Claridge J B, Darling G R and Rosseinsky M J 2003 *Phys. Rev.* B **67** 245106

[10] An J M, Rosner H, Savrasov S. Y and Pickett W E 2003 *Physica* B **328** 1

[11] Lee K W and Pickett W E 2003 *Phys. Rev.* B **68** 085308

[12] Liu Z L, Chen X R and Wang Y L 2006 *Physica* B **381** 139

[13] Kobayashi K and Arai M 2003 *Physica* C **201** 388

[14] Ponomarenko O, Radny M W and Smith P V 2007 *Phys. Rev.* B **76** 035414

[15] Lazicki A, Yoo C S, Cynn H, Evans W J, Pickett W E, Olamit J, Liu K and Ohishi Y 2007 *Phys. Rev.* B **75** 054507

[16] Hinks D G, Claus H and Jorgensen J D 2001 *Nature* **411** 457

[17] Hohenberg P and Kohn W 1964 *Phys. Rev.* B **136** 864

[18] Kohn W and Sham L 1965 *Phys. Rev.* A **140** 1133

[19] Blaha P, Schwarz K, Madsen G K H, Kvasnicka D and Luitz J 2001 WIEN2K, an augmented plane wave plus local orbitals program for calculating crystal properties (Vienna: Vienna University of Technology)

[20] Perdew J P, Burke K and Ernzerhof M 1996 *Phys. Rev. Lett.* **77** 3865

[21] Perdew J P and Wang Y 1992 *Phys. Rev.* B **45** 13244

[22] Blanco M A, Francisco E and Luana V 2004 *Comput. Phys. Commun.* **158** 57-72

[23] Blanco M A, Martín Pendás A, Francisco E, Recio J M and Franco R 1996 *J. Mol. Struct.* (*Theochem.*) **368** 245

[24] FlÓrez M, Recio J M, Francisco E, Blanco M A and Pendás A M 2002 *Phys. Rev.* B **66** 144112

[25] Vogel D, Kruger P and Pollmann J 1997 *Phys. Rev.* B **55** 12836

[26] Pugh S K, Dugdale D J, Brand S and Abram R A 1999 *Semicond. Sci. Technol.* **14** 23

[27] Francisco E, Recio J M, Blanco M A and Martín Pendás A 1998 *J. Phys. Chem.* **102** 1595

[28] Francisco E, Blanco M A and Sanjurjo G 2001 *Phys. Rev.* B **63** 094107

[29] Chen X R, Li X F, Cai L C and Zhu J 2006 *Solid State Commun.* **139** 246

[30] Zhou X L, Liu K, Chen X R and Zhu J 2006 *Chin. Phys.* **15** 3014

[31] Lu L Y, Chen X R, Yu B R and Gou Q Q 2006 *Chin. Phys.* **15** 0802

[32] Li X F, Chen X R, Meng C M and Ji G F 2006 *Solid State Commun.* **139** 197

[33] Cheng Y, Lu L Y, Jia O H and Chen X R 2008 *Chin. Phys.* **17** 1355

[34] Baonza García V, Cáceres M and Núñez J 1995 *Phys. Rev.* B **51** 28

[35] Ravindran P, Vajeeston P, Vidya R, Kjekshus A and Fjellvåg H 2001 *Phys. Rev.* B **64** 224509

[36] Choi H J, Roundy D, Sun H, Cohen M L and Louie S G 2002 *Nature* **418** 758

[37] Blochl P E, Jepsen O and Andersen O K 1994 *Phys. Rev.* B **49** 16223